Dielectric Constant and Density Dependence of the Structure of Supercritical Carbon Dioxide Using a New Modified Empirical Potential Model: A Monte Carlo Simulation Study

Yang Zhang, Jichu Yang,† and Yang-Xin Yu*,‡

Department of Chemical Engineering, Tsinghua University, Beijing 100084, People's Republic of China

Received: September 20, 2004; In Final Form: May 20, 2005

Two modified versions of the Elementary Physical Model (EPM) [*J. Phys. Chem.* **1995**, *99*, 12021] for supercritical carbon dioxide have been proposed in this work and their validities are affirmed by computing the thermodynamic properties and dielectric constant up to 910 kg/m^3 with use of canonical ensemble Monte Carlo simulation. Simulations performed for 500 molecules with the EPM2-M model reproduce the experimental data accurately at all thermodynamic states. The structural analyses demonstrate that the aggregation is strong at low density while the coordination number is large at high density. In addition, a detailed study on the radial and angular correlation functions reveals that the T-shaped geometry is dominate while a variety of other structures still appear in the first coordination shell. Furthermore, the angular correlation functions show that the probability of a molecule being oriented toward the convex side of another molecule is equal to that pointing toward the concave side since the molecular nonlinearity of carbon dioxide is only marginal. As the distance between two molecules increases, the preferred orientations disappear quickly and all the results are in good agreement with the prior ab initio calculation [*J. Chem. Phys.* **2004**, *120*, 9694].

I. Introduction

Carbon dioxide is often promoted as a "green" solvent since it is a resourceful, low toxic, and nonflammable fluid.[1] Furthermore, carbon dioxide is widely used to increase reaction rates and develop efficient separation processes under supercritical conditions.[1−3]

To obtain detailed information on structural and thermodynamic properties of supercritical fluids, experimental and theoretical studies as well as molecular simulations have been carried out for decades. Span et al.[4] reviewed the available data on thermodynamic properties of carbon dioxide and developed an equation of state capable of reproducing the experimental data up to 800 MPa and 1100 K. Several experiments on the fluid structures (e.g., X-ray and neutron diffraction experiments) covering many different regions of the density−temperature plane (including liquid, gas, and supercritical states) have been reported.[5−9] Besides experimental and theoretical studies, molecular simulation provides us an alternative way to study the thermodynamic and structural properties. Using Monte Carlo simulation, Colina et al.[10] investigated the thermodynamic properties of carbon dioxide. The pair correlation functions have also been studied using molecular simulation for many years. However, the behavior of supercritical carbon dioxide, especially for the detailed structure at high density and pressure, has not been investigated until recently.[5,6]

In molecular simulations, a reliable potential is indispensable for obtaining accurate thermodynamic and structural properties. Up to now, there have been a considerable number of potentials developed for carbon dioxide. The potential models can be divided into two groups according to their origins. The first group includes two-body or three-body empirical models,[11−16] and the second group is based on ab initio quantum mechanical calculations.[17−19] The empirical potentials are more popular because of their simple forms and excellent calculation accuracy. In most empirical models, a carbon dioxide molecule is treated as a linear one with a large quadrupole moment. However, according to current ab initio calculations[19,20] and neutron diffraction experiments,[6,8] a supercritical carbon dioxide molecule is marginally nonlinear. In this study, this nonlinearity is introduced to the original EPM models.[13] Thus, a supercritical carbon dioxide molecule in the new modified models has a large quadrupole moment and a small dipole moment. As a result, the dielectric constant is not equal to a unit anymore.

The main purpose of this work is to affirm the reliabilities of the new modified models by reproducing the thermodynamic properties and dielectric constant of carbon dioxide over a wide range of density. After that, both the radial and orientational structures are investigated in detail with use of the optimized model. Different from previous investigations which mainly focused on the gas-state carbon dioxide,[21,22] this work simulates the density dependence of structure in supercritical CO_2.

The rest of the paper is organized as follows. In Section II, we briefly describe the computational details and model developments. Section III contains the main results. In particular, in Section IIIA,B, the reliabilities of the new models are tested and the dielectric constant at different thermodynamic states is calculated, while in Section IIIC−E the molecular aggregation and spatial structures are analyzed in detail. Finally, Section IV concludes with a few general remarks.

II. Molecular Models and Simulation Details

A. Model and Potential Function. Many of the latest investigations on supercritical carbon dioxide have shown that its structure has a marginal deviation from the linear geometry.[6,8,19,20] In a very recent Car−Parrinello molecular dynamics

† E-mail: yjc-dce@mail.tsinghua.edu.cn.
‡ E-mail: yangxyu@mail.tsinghua.edu.cn.

10.1021/jp045741r CCC: $30.25
Published on Web 06/21/2005

TABLE 1: Potential Function Parameters for Carbon Dioxide

EPM-modified model					
ϵ_{C-C}/k_B	28.999 K	σ_{O-O}	3.064 Å	l_{C-O}	1.161 Å
σ_{C-C}	2.785 Å	ϵ_{C-O}/k_B	49.060 K	q_C[a]	+0.6645 e
ϵ_{O-O}/k_B	82.997 K	σ_{C-O}	2.921 Å		
EPM2-modified model					
ϵ_{C-C}/k_B	28.129 K	σ_{O-O}	3.033 Å	l_{C-O}	1.149 Å
σ_{C-C}	2.757 Å	ϵ_{C-O}/k_B	47.588 K	q_C	+0.6512 e
ϵ_{O-O}/k_B	80.507 K	σ_{C-O}	2.892 Å	k_θ	1236 kJ/mol/rad^2

[a] q_c is the charge on the carbon center; there are two equal negative charges on the oxygen centers.

simulation study,[20] it is found that the intramolecular bond angle $\theta = 174.2°$ at 318.15 K and 703 kg/m^3. To build more reliable empirical models for the supercritical fluid, the nonlinearity is embedded in the well-known elementary physical models (EPM).[13] The new modified models are called the EPM-modified model (EPM-M) and EPM2-modified model (EPM2-M). Moreover, the EPM-M is a completely rigid model while EPM2-M has a flexible bond angle and a fixed bond length.

The original EPM models have been successfully applied to the investigations of pure carbon dioxide and its mixtures.[23−26] The critical temperatures predicted from the EPM and EPM2 models are 313.4 and 304.2 K, respectively, which are rather close to the experimental value (304.2 K).[13] The potential parameters of the new models are listed in Table 1. All the values of the potential parameters are the same as those in the original EPM models except for the intramolecular bond angle ($\theta_0 = 174.2°$). The bond stretching potential in the flexible model is defined as

$$u(\theta) = \frac{1}{2}k_\theta(\theta - \theta_0)^2 \tag{1}$$

where k_θ, θ, and θ_0 are the force constant, bending angle, and equilibrium bending angle, respectively. The intermolecular potential energy between two carbon dioxide molecules is given by

$$u(1,2) = u_{LJ}(1,2) + u_{Coul}(1,2) = \sum_{i\in\{1\}}\sum_{j\in\{2\}}\left\{4\epsilon_{ij}\left[\left(\frac{\sigma_{ij}}{r_{ij}}\right)^{12} - \left(\frac{\sigma_{ij}}{r_{ij}}\right)^{6}\right] + \frac{1}{4\pi\epsilon_0}\frac{q_iq_j}{r_{ij}}\right\} \tag{2}$$

where i and j are the interaction sites on two different molecules 1 and 2, respectively. r_{ij} denotes the distance between two interaction sites i and j. ϵ_0 is the permittivity of vacuum and q_i is the charge while ϵ_{ij} and σ_{ij} are the Lennard-Jones parameters shown in Table 1. Although the Ewald summation method can be used to estimate the long-range electrostatic interactions with results similar to that from the reaction field method,[23,27−29] it is computationally expensive.[27,28] Therefore, the reaction field method is selected to handle the long-range electrostatic forces in this work. In this method, the long-range interaction is given by

$$U_{Coul} = \sum_{i\in\{1\}}\sum_{j\in\{2\}} q_iq_j\left[\frac{1}{r_{ij}} + \frac{\epsilon_{rf}-1}{2\epsilon_{rf}+1}\frac{{r_{ij}}^2}{{r_{cut}}^3} - \left(\frac{1}{r_{cut}} + \frac{\epsilon_{rf}-1}{2\epsilon_{rf}+1}\frac{{r_{cut}}^2}{{r_{cut}}^3}\right)\right] \tag{3}$$

where ϵ_{rf} and r_{cut} denote the reaction field dielectric constant and the cutoff distance, respectively. ϵ_{rf} is assumed to be infinity and this conducting boundary ($\epsilon_{rf} = \infty$) leads to both reasonably consistent results and good computational efficiency.[27,28]

B. Dielectric Constant. In the new modified EPM models, each carbon dioxide molecule possesses not only a quadrupole moment but also a small dipole moment. This dipole moment is related to the finite system Kirkwood g-factor[28] through

$$\frac{(\epsilon - 1)(2\epsilon_{rf}+1)}{(2\epsilon_{rf}+\epsilon)} = 3yG_k(\epsilon_{rf}) \tag{4}$$

where $y = 4\pi\rho_n\mu^2/9k_BT$. ρ_n is the number density and μ is the dipole moment of a single molecule. k_B is Boltzmann constant and T is the temperature while G_k is calculated in a simulation by

$$G_k = \frac{\langle M^2\rangle - \langle M\rangle^2}{N\mu^2} \tag{5}$$

where M and N are the total dipole moment and the number of molecules in the simulation box. As a result, under the conducting boundary condition, eq 4 reduces to

$$\epsilon = \epsilon_\infty + \frac{4\pi}{3kT\langle V\rangle}(\langle M^2\rangle - \langle M\rangle^2) \tag{6}$$

In eq 6, V is the volume of the simulation box and ϵ_∞ is the infinite frequency, which is equal to 1 for these nonpolarizable models. The $\langle M\rangle^2$ term in eqs 5 and 6 is neglected since the ensemble average of the total dipole moment is close to zero after a long simulation time.[28,30,31] It should be pointed out that eq 6 is frequently used in the dielectric constant calculation for both high and weak polar liquids.[21,24,28−30]

C. Simulation Details. The standard canonical ensemble (NVT) Monte Carlo (MC) simulations are carried out in this work. The carbon dioxide molecules are placed in a cubic box with periodic boundary conditions. To verify that the results are independent of the size of the system, simulations containing 256, 500, and 864 molecules are performed at different densities. The simulation results show that 500 molecules are enough to obtain accurate results. The cutoff distance is equal to half of the simulation box length. Long-range corrections to the Lennard-Jones potential due to the truncation of interactions are calculated by using the traditional statistical mechanical equations.[27] There are two kinds of molecular movements inside the simulation box: translation and rotation. The acceptance ratios of both movements are adjusted to 50% in the simulations. At least 3×10^5 MC cycles are used for the sampling period after 2×10^5 MC cycles for system equilibration. The errors during simulation are estimated by the block method.[32]

III. Results and Discussion

A. Reliability of the Model. One of the most important issues in computer simulation is to choose or build a reliable potential model. Before further calculations and discussions could be done, it was obligatory to check if the potential model could reproduce experimental data accurately. Therefore, the reliabilities of the EPM-M and EPM2-M models are affirmed by simulating the pressure and internal energy as a function of density at three temperatures: 313.15, 333.15, and 353.15 K. The internal energies have been simulated by Kolafa et al.[24] with the EPM2 model and our results are consistent with their work. Therefore, we only give the simulation results of pressures in Figure 1. From Figure 1, one can see that the EPM-M gives slightly more accurate results than the EPM2-M does at low

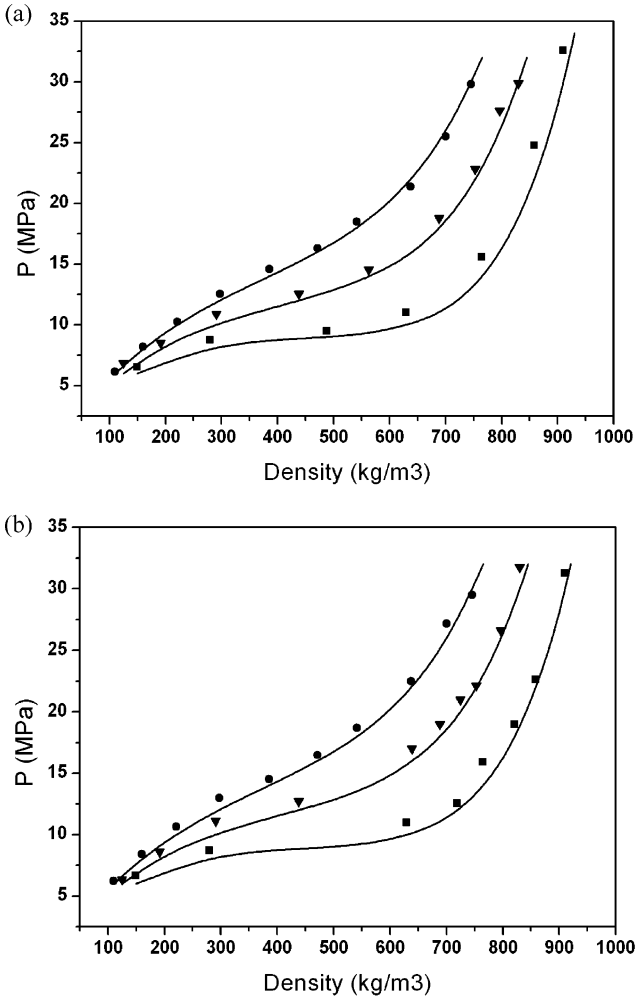

Figure 1. Pressure as a function of density at 313 (■), 333 (▼), and 353 K (●): (a) EPM-M model and (b) EPM2-M model. The solid lines represent the experiment results taken from ref 33.

density, while the EPM2-M model performs better in the high-density region. Since there is very little difference between parts a and b of Figure 1, it can be judged that the flexible bond angle in carbon dioxide does not affect some of the thermodynamic properties in an obvious fashion. Despite some minor defects, the new modified EPM models can reproduce experimental data very well. To further demonstrate the reliabilities of the new models, the dielectric constant is also calculated in the following section.

B. Dielectric Constant. The dielectric constant is not only closely related to the macroscopic properties such as solubility, reaction rate constant, etc., but has a strong dependence on the microscopic molecular orientational distribution as well. The static dielectric constant of supercritical carbon dioxide at different temperatures is computed by using eq 6 and compared with experimental data (ref 33) in Figure 2. Simulation errors are within 5% and 3% for pressure and dielectric constant, respectively.

Figure 2 shows that the dielectric constant decreases as temperature increases, which suggests that the molecular ordering is weak at the high-temperature region. In Figure 2a, there are obvious deviations between simulation results and experimental data at high pressure. The simulation results are notably smaller than experimental values. As expected, results from the EPM2-M model show good agreement with experimental data at all states as shown in Figure 2b. However, bond angle distribution apparently does not change with the EPM2-M model

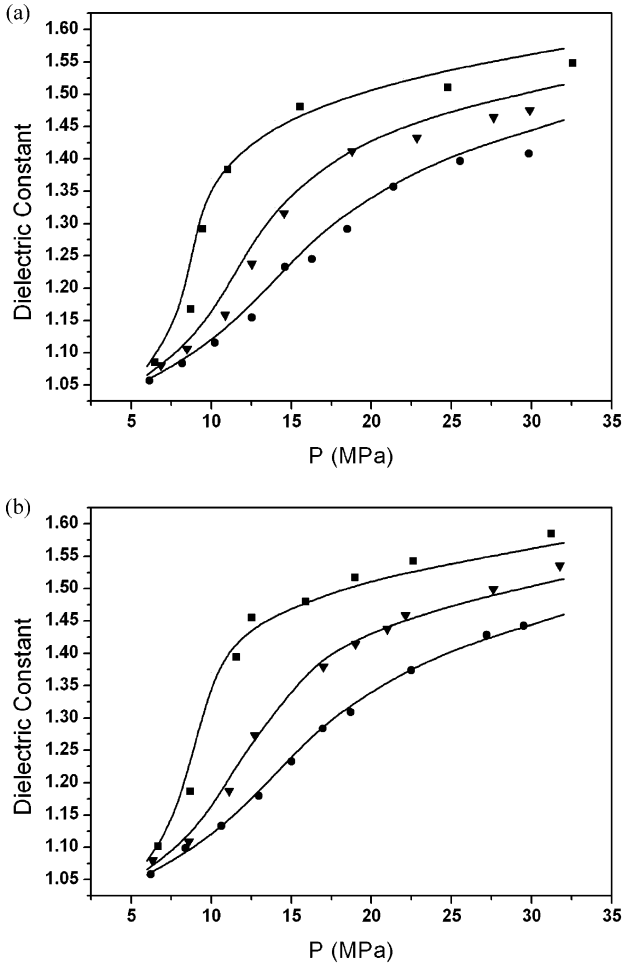

Figure 2. Dielectric constant as a function of pressure at 313 (■), 333 (▼), and 353 K (●): (a) EPM-M model and (b) EPM2-M model. The solid lines represent the experimental results taken from ref 33.

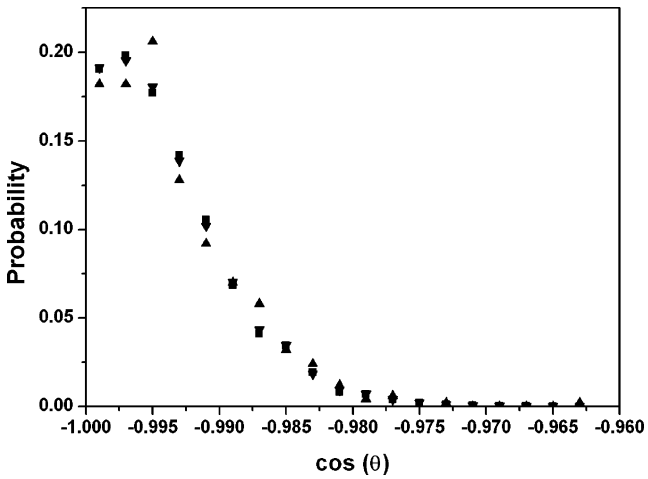

Figure 3. Intramolecular angular distribution at three different states: $T = 313$ K, $\rho = 149.2$ kg/m^3 (■); $T = 313$ K, $\rho = 910.4$ kg/m^3 (▼); and $T = 353.15$ K, $\rho = 745.5$ kg/m^3 (▲).

at different states (Figure 3) according to our simulations, which indicates that the intermolecular bond angle distribution is the main factor affecting dielectric constant. It should be pointed out here that ρ in Figures 3 and 4 represents the density of carbon dioxide. From Figure 2, it can be concluded that the flexible model is more reliable than the completely rigid one, especially at high density. Consequently, the EPM2-M model is selected in the following investigations on the structures of supercritical fluid.

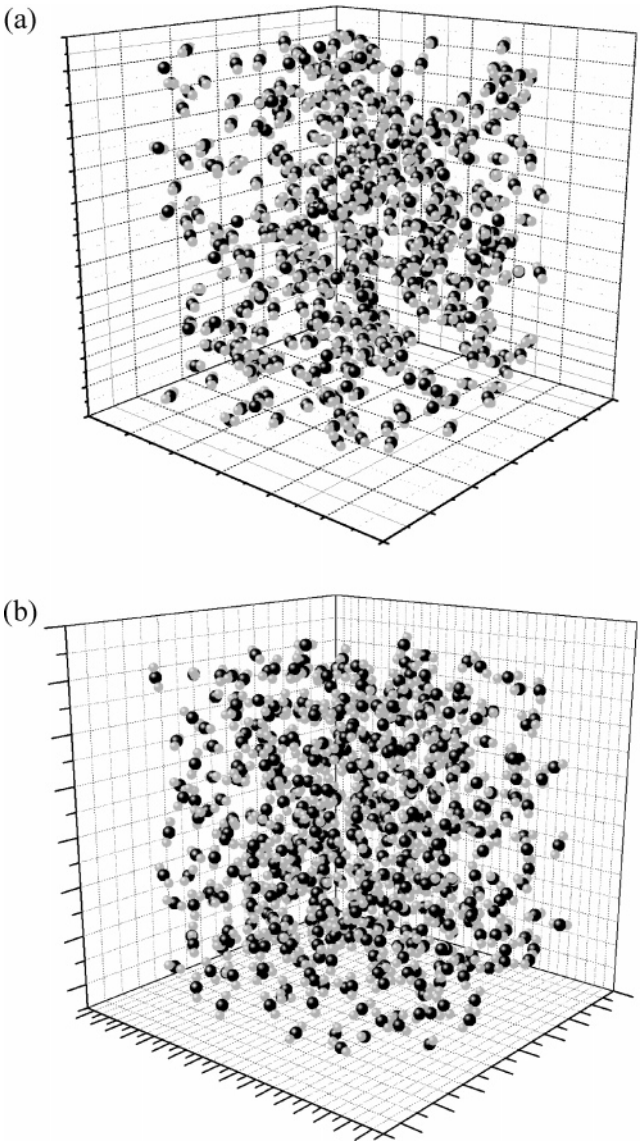

Figure 4. Snapshots of the configuration of 500 molecules of supercritical carbon dioxide obtained by Monte Carlo calculations. Oxygen atoms are shown in gray, and carbon atoms are in black. (a) Box length = 61.1 Å, T = 353 K, ρ = 160.1 kg/m^3; (b) box length = 36.6 Å, T = 353 K, ρ = 745.5 kg/m^3.

C. Aggregation of Supercritical Carbon Dioxide. The structures of supercritical fluid have been studied for more than 10 years.[5−9] In particular, Ishii et al.[6] reported the density dependence of the structure of supercritical carbon dioxide recently. However, the potential models used in these simulations are two-center Lennard-Jones plus point quadrupole models or three-center linear Lennard-Jones models. Thus, by applying the new modified EPM2-M model, one can expect to obtain detailed information and accurate results.

To visualize the aggregation phenomena (local density inhomogeneity) in supercritical carbon dioxide, snapshots of the fluid at two different densities along an isotherm (353.15 K) are shown in Figure 4. At a high density (ρ = 745.5 kg/m^3), the structure of molecules shows very small local density inhomogeneity since the molecules are very densely arranged. In contrast, at a relatively low density (ρ = 160.1 kg/m^3), the aggregation is more obvious. Large clusters can be found in the three-dimensional figure (Figure 4a), which suggest a strong local density inhomogeneity. These observations agree with the earlier MD and neutron scattering measurement results reported by Ishii et al.[6,8] Hereby, in supercritical carbon dioxide, as the fluid density increases, the local density inhomogeneity decreases. These results demonstrate that the fluid structure at low density is dominated by the attractive forces. To quantitatively describe the local density inhomogeneity, the coordination numbers are calculated from

$$N_C = 4\pi\rho_n \int_0^{r_{min}} g(r) r^2 \, dr \qquad (7)$$

where $g(r)$ is the pair correlation function and r_{min} is the radial distance corresponding to the first minimum of $g(r)$. The calculated coordination numbers are listed in Table 2.

TABLE 2: Pair Correlation Functions and Coordination Numbers at 313 K and Different Densities

density, kg/m^3	quantity	CC	CO	OO
149.2	1st maximum of RDF, Å	4.4	4.5	3.8
	1st minimum of RDF, Å	6.3	6.8	4.5
	coordination no.	3.1	6.0	2.2
910.4	1st maximum of RDF, Å	4.2	4.2	3.5
	1st minimum of RDF, Å	6.2	6.2	4.5
	coordination no.	12.8	25.1	8.0

D. Pair Correlation Functions. There are three representative geometries shown in Figure 5: the slipped-parallel, T-shaped, and crossed geometries.[24] The C−C separation is about 3.6 Å for the slipped-parallel structure, 4.2 Å for the T-shaped geometry, and 3 Å for the crossed shape. According to the minimum-energy gas-phase structure calculation and neutron scattering experiments, it has been generally accepted[21,24,34] that the carbon dioxide dimer has a slipped-parallel geometry. The T-shaped configuration is a metastable state, the energy of which is almost the same as that of the slipped-parallel geometry. However, when we focus on the supercritical fluid structures, the T-shaped geometry is dominant especially at high density.[5,6,20,21,24] To study the radial and orientational structure, two-dimensional spatial−angular correlation functions are comprehensively investigated with the EPM2-M model in Sections D and E.

Since temperature does not affect the pair distribution functions greatly ranging from 313 to 353 K, we focus on the density dependence of the structure. Figure 6 shows the pair correlation functions at 313 K and four different densities (149.2 279.9, 629.3, 910.4 kg/m^3). For the convenience of comparison, the curves are not shifted. Table 2 summaries the maximum, minimum positions of the first peak and the coordination numbers at two different densities. Figure 6a displays the radial distribution function (RDF) between two carbon atoms, g_{CC}, and the first maximum peak locates at around 4.2 to 4.4 Å. Since the crossed geometry has a C−C separation of about 3 Å, it can be concluded that very few molecules hold this shape in the system. The broad peak at 149.2 kg/m^3 indicates that there exist a number of different orientational arrangements. Furthermore, the first peak in g_{CC} is marginally shifted with incremental changes in density. At 910.4 kg/m^3, the first peak becomes narrower and the maximum lies at 4.2 Å, which means that the T-shaped geometry is dominant and the broad peak again indicates different geometries appear. Table 2 supports that the coordination number is larger at high density although the maximum in the pair correlation function is lower for high-density fluid. To find out which configuration is dominant in a more explicit way, two-dimensional radial−angular correlation functions are calculated and discussed in the following sections.

From Figure 6b, it can be seen that the first peak of RDF between carbon and oxygen, g_{CO}, is very broad at low density, which is identical with g_{CC}. Meanwhile, at high density, there

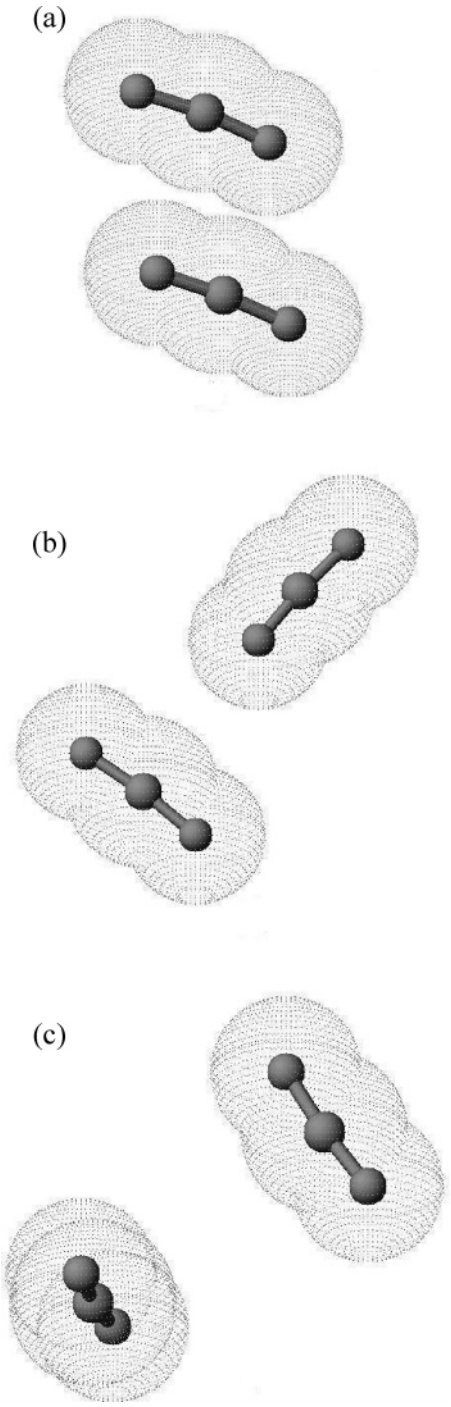

Figure 5. Configurations of supercritical carbon dioxide dimer: (a) slipped-parallel, (b) T-shaped, and (c) crossed.

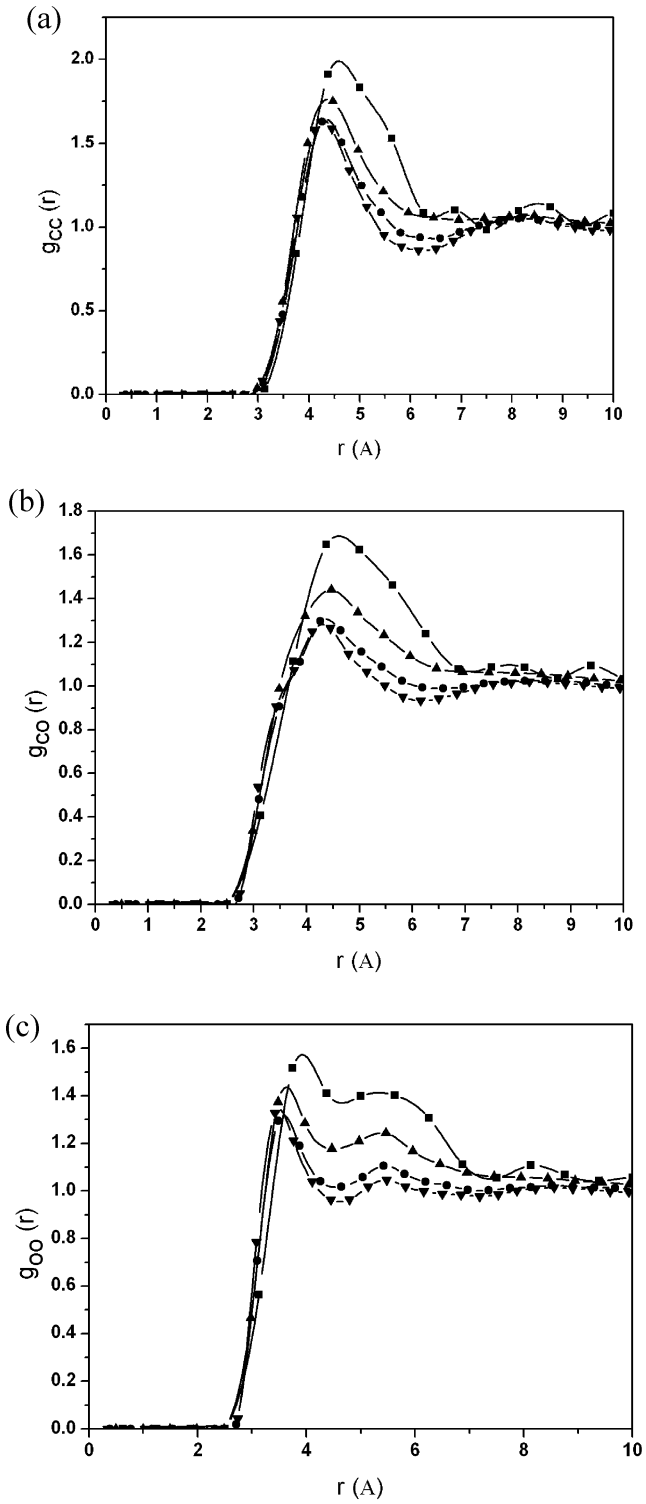

Figure 6. Pair correlation functions for supercritical carbon dioxide predicted from the EPM2-M model at four different densities along an isotherm (313 K): 149.2 (■), 279.9 (▲), 629.3 (●), and 910.4 kg/m^3 (▼); (a) g_{CC}, (b) g_{CO}, and (c) g_{OO}.

are changes in the slope of g_{CO} at around 3.5 Å, which means the structure of the fluid is highly ordered. The position of first maximum, minimum of g_{CO} and the coordination numbers are listed in Table 2. It is likely that most carbon atoms within the distance $r = 6.5$ Å share the other two oxygen atoms of the molecule within the first coordination shell. Saharay et al.[20] found a similar result through ab initio study recently. In their work, the first maxima and minima of g_{OO} are consistent with the discussion of g_{CC} and g_{CO} described above. The different trends of change in Figure 6c also support that the supercritical carbon dioxide is gaslike at low density and liquidlike at high density along an isotherm.

E. Orientational Distribution. Cipriani et al.[5] and Kolafa et al.[24] have predicted that the supercritical carbon dioxide molecules in the first coordination shell lay in the equatorial plane of the central molecule. To affirm this and obtain further structural information, we used a method similar to that of Fedchenia et al.[21] At first, the relative position between two molecules is described in Figure 7. Each molecule has its own orientations which are depicted by X, Y, and Z axes. The X axis is along the dipole moment direction. The Y axis is perpendicular to the X axis and belongs to the molecular plane (O−O direction). The Z axis is perpendicular to the molecular

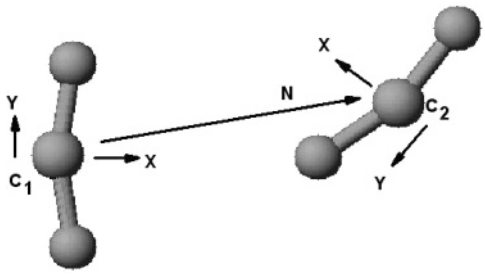

Figure 7. Relative position between two interaction molecules for the calculation of radial−angular correlation functions in supercritical carbon dioxide.

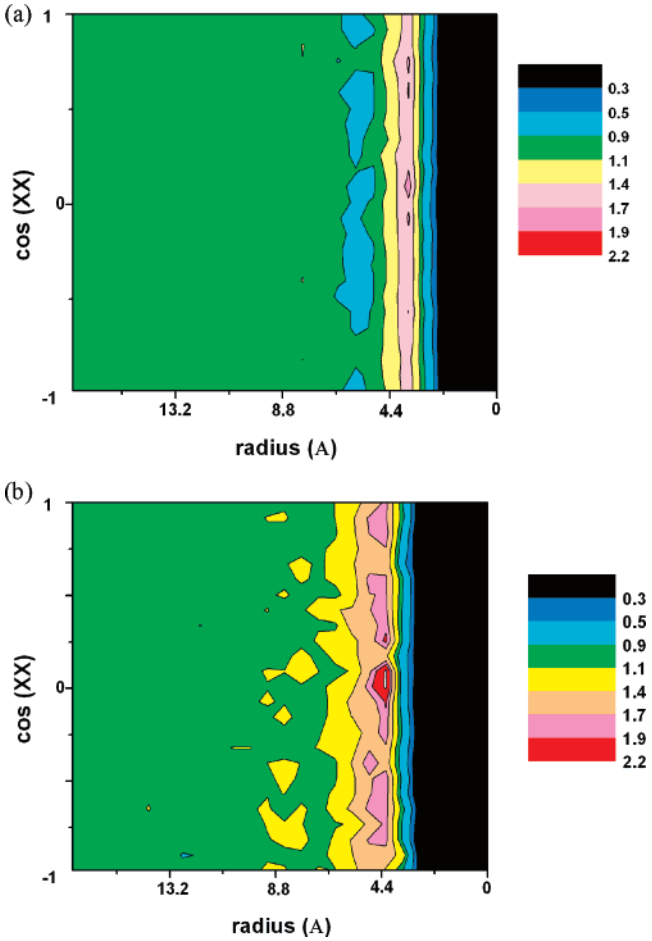

Figure 8. Isoprobability contour map of radius and cos(XX) at two thermodynamic states: (a) $T = 313$ K, $\rho = 910.4$ kg/m^3 and (b) $T = 313$ K, $\rho = 279.9$ kg/m^3.

plane while the N axis is along the C_1-C_2 direction. Through the calculation of cos(XX), cos(XN), and the radial distance between each pair of molecules, we could obtain the two-dimensional radial−angular correlation functions of the system.

Figures 8 and 9 show that the correlations between cos(XX) and cos(XN) at two representative thermodynamic states: 910.4 kg/m^3, 313 K and 279.9 kg/m^3, 313 K, which represent the liquidlike high-density and gaslike low-density fluids, respectively. In Figures 8 and 9, the radial axis represents the distance between two carbon atoms. In Figure 8, for both high- and low-density liquids, the highest level of probability appears at around $r = 4.2$ Å and cos(XX) = 0. These results suggest that the dipoles of each pair of molecules are perpendicular to each other. There are two maxima in Figure 9 which appear at $r = 4.2$ Å and cos(XN) = −1, 1. Another small peak is located at $r = 4.2$

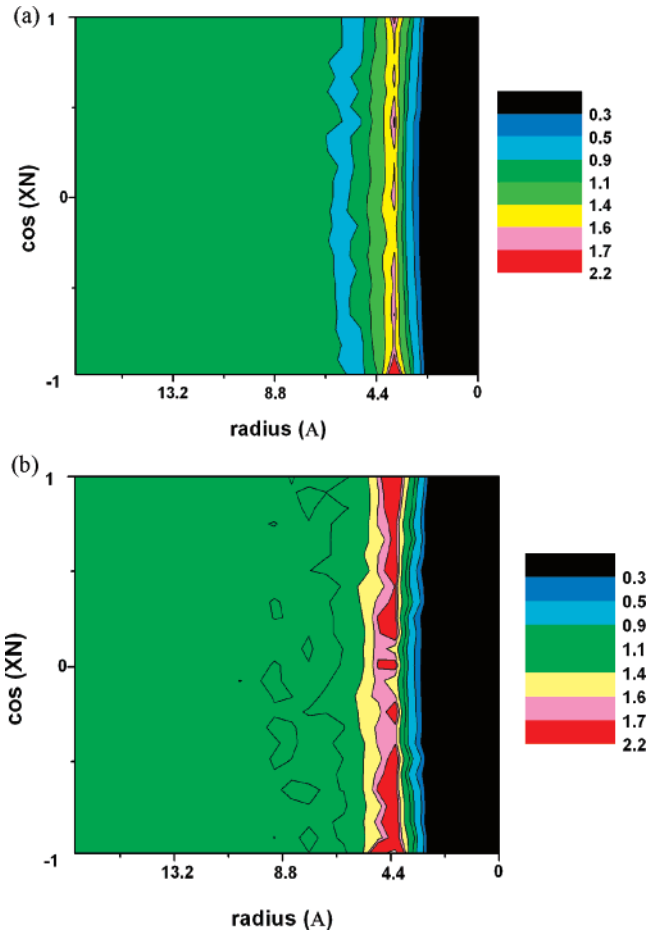

Figure 9. Isoprobability contour map of radius and cos(XN) at two thermodynamic states: (a) $T = 313$ K, $\rho = 910.4$ kg/m^3 and (b) $T = 313$ K, $\rho = 279.9$ kg/m^3.

Å and cos(XN) = 0, which means the molecules hold the T-shaped or crossed geometry. Furthermore, when the radial distance is taken into account, the crossed orientation (C−C maximum is around 3 Å) is not preferred. Meanwhile, from Figures 8 and 9, one can see that these preferred orientations do not exist beyond the first coordination shell, which means the strong preferred orientations disappear rather quickly as the distance increases.

With density decreasing, the main trends of change in Figures 8 and 9 are almost the same. The coordination shell at 279.9 kg/m^3 is not as obvious as that of 910.4 kg/m^3 while the first peak at a lower density is more prominent than that at a higher density, which is in accord with Figure 6. Moreover, at low density, the first peak in the correlation function is broad, which means many different structures other than T-shape appear. These two-dimensional correlation functions are consistent with the analysis in section D and support that the structure is less ordered and the many body effect is more distinct at low density.[20]

Figure 10 is introduced to depict the orientational structure in a more explicit way. The X, Y axes are cos(XN) and cos(XX), respectively, and the Z axis is the probability of the corresponding distribution. In our calculation, all the molecules in the first coordination shell are taken into account. The cos(XN)−cos(XX) correlation functions at different densities are really identical with each other, thus the orientational structure within the first coordination shell is less relevant to the system density. The three maxima locate at cos(XN) = −1, 0, 1 and

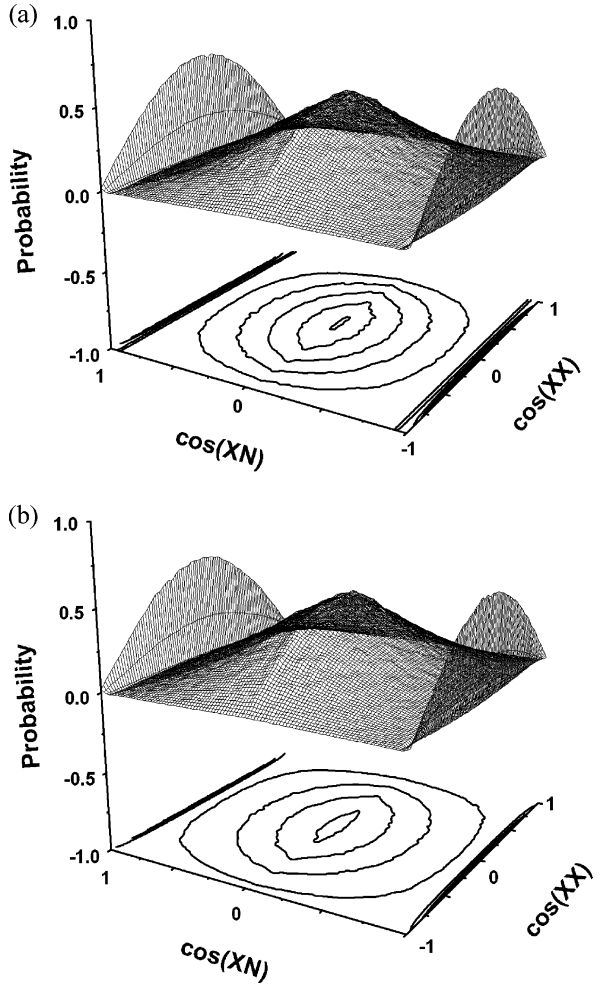

Figure 10. Isoprobability contour map of cos(XX) and cos(XN) at two thermodynamic states: (a) $T = 313$ K, $\rho = 910.4$ kg/m^3 and (b) $T = 313$ K, $\rho = 279.9$ kg/m^3.

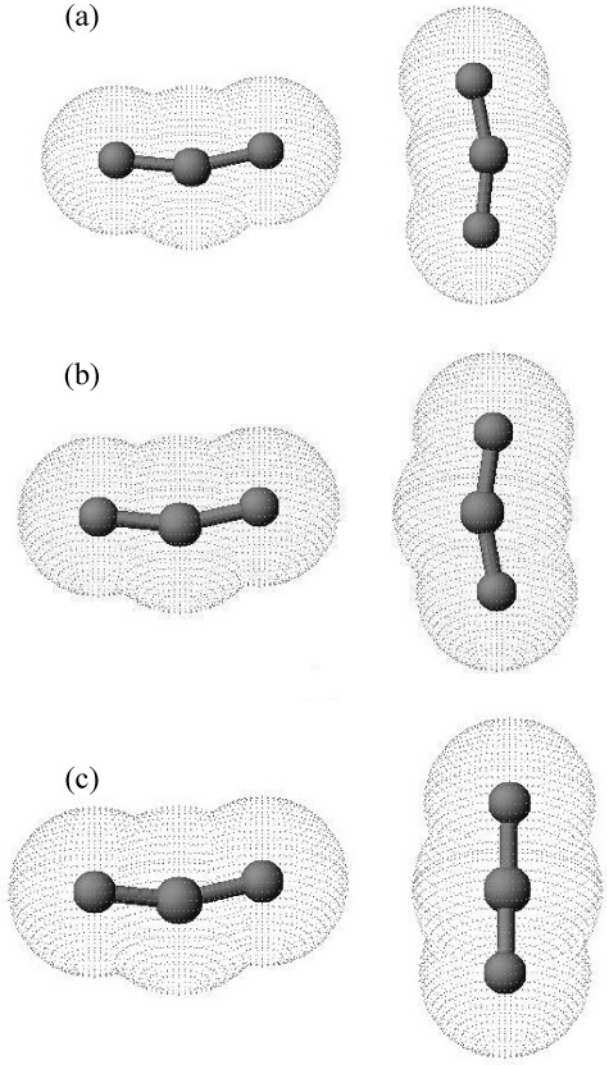

Figure 11. Three representative T-shaped structures: (a) concave; (b) convex; and (c) perpendicular.

cos(XX) = 0. Again, the correlation functions suggest that the T-shaped and crossed geometries are dominant. After ruling out the crossed geometry, three characteristic T-shaped structures are shown in Figure 11, which are called concave (a molecule oriented toward the concave side of another molecule), convex (a molecule oriented toward the convex side of another molecule), and perpendicular geometries, respectively. Meanwhile, the broad peak in Figure 10 indicates that there exist a number of different orientations. The correlation functions at cos(XN) = −1 and 1 are identical with each other, which suggests that the possibilities of concave and convex geometries are the same. Similar results have been found in the investigations on water structure,[35,36] but the concave structure is preferred to convex geometry[36] in that case. We do not observe this preferred structure in our simulations, probably since the structure of the carbon dioxide molecule is nearly linear.

IV. Conclusions

In our newly developed empirical models, supercritical carbon dioxide is regarded as a nonlinear molecule. Standard Monte Carlo simulations in the canonical ensemble (NVT) have been performed to test the three-site, fixed-charge models (EMP-M and EPM2-M) with emphasis on reproducing the thermodynamic properties and dielectric constant. The flexible model (EPM2-M) predicts the thermodynamic data pretty well. Moreover, EPM2-M model is able to calculate the dielectric constant with good computational accuracy over a wide range of thermodynamic states. The pair correlation functions qualitatively agree with neutron diffraction experiments and other simulation results. At low density, the structure is dominated by the attractive forces while at high density it is determined by the repulsive forces. The T-shaped geometry is dominant at different densities through the analysis of radial−angular correlation functions. Finally, we find the concave and convex T-shaped geometries are equally preferred in the first coordination shell. The preferred orientations disappear quickly as distance increases. All these results are consistent with Saharay's work, which indicates that supercritical carbon dioxide possesses a small dipole moment. Overall, the EPM2-M model shows a significant improvement in dielectric constant calculation.

The nonzero dipole and large quadrupole moments have a strong effect on the solubility and reaction rates in supercritical fluids. Additional studies on the solubility and aggregation of alcohols in supercritical carbon dioxide are being undertaken. To understand the molecular interactions and their dependence on macroscopic phenomena is the main goal of our future endeavors.

Acknowledgment. We thank the reviewers for their helpful suggestions. This work was supported by the National Natural Science Foundation of China under Grant No. 20376037.

References and Notes

(1) Beckman, E. J. *J. Supercrit. Fluids* **2004**, *28*, 121.
(2) Baiker, A. *Chem. Rev.* **1999**, *99*, 453.
(3) Turner, C. H.; Gubbins, K. E. *J. Chem. Phys.* **2003**, *119*, 6057.
(4) Span, R.; Wagner, W. *J. Phys. Chem. Ref. Data* **1996**, *25*, 1509.
(5) Cipriani, P.; Nardone, M.; Ricci, F. P.; Ricci, M. A. *Mol. Phys.* **2001**, *99*, 301.
(6) Ishii, R.; Okazaki, S.; Okada, I.; Furusaka, M.; Watanabe, N.; Misawa, M.; Fukunaga, T. *J. Chem. Phys.* **1996**, *105*, 7011.
(7) Morita, T.; Nishikawa, K.; Takematsu, M.; Iida, H.; Furutaka, S. *J. Phys. Chem. B* **1997**, *101*, 7158.
(8) Ishii, R.; Okazaki, S.; Odawara, O.; Okada, I.; Misawa, M.; Fukunaga, T. *Fluid Phase Equil.* **1995**, *104*, 291.
(9) Ishii, R.; Okazaki, S.; Okada, I.; Furusaka, M.; Watanabe, N.; Misawa, M.; Fukunaga, T. *Chem. Phys. Lett.* **1995**, *240*, 84.
(10) Colina, C. M.; Olivera-Fuentes, C. G.; Siperstein, F. R.; Lisal, M.; Gubbins, K. E. *Mol. Simul.* **2003**, *29*, 405.
(11) Moller, D.; Fischer, J. *Fluid Phase Equil.* **1994**, *100*, 35.
(12) Murthy, C. S.; Singer, K.; McDonald, I. R. *Mol. Phys.* **1981**, *44*, 135.
(13) Harris, J. G.; Yung, K. H. *J. Phys. Chem.* **1995**, *99*, 12021.
(14) Kobashi, K.; Kihara, T. *J. Chem. Phys.* **1980**, *72*, 3216.
(15) Vrabec, J.; Stoll, J.; Hasse, H. *J. Phys. Chem. B* **2001**, *105*, 12126.
(16) Potoff, J. J.; Siepmann, J. I. *AIChE J.* **2001**, *47*, 1676.
(17) Steinebrunner, G.; Dyson, A. J.; Kirchner, B.; Huber, H. *J. Chem. Phys.* **1998**, *109*, 3153.
(18) Bukowski, R.; Sadlej, J.; Jeziorski, B.; Jankowski, P.; Szalewicz, K.; Kucharski, S. A.; Williams, H. L.; Rice, B. M. *J. Chem. Phys.* **1999**, *110*, 3785.
(19) Shkrbo, I. A. *J. Phys, Chem. A* **2002**, *106*, 11871.
(20) Saharay, M.; Balasubramanian, S. *J. Chem. Phys.* **2004**, *120*, 9694.
(21) Fedchenia, I. I.; Schroder, J. *J. Chem. Phys.* **1997**, *106*, 7749.
(22) Stassen, H.; Dorfmuller, Th.; Ladanyi, B. M. *J. Chem. Phys.* **1994**, *100*, 6318.
(23) Kettler, M.; Nezbeda, I.; Chialvo A. A.; Cummings, P. T. *J. Phys. Chem. B* **2002**, *106*, 7537.
(24) Kolafa, J.; Nezbeda, I.; Lisal, M. *Mol. Phys.* **2001**, *99*, 1751.
(25) Chatzis, G.; Samios, J. *Chem. Phys. Lett.* **2003**, *374*, 1267.
(26) Rocha, S. R. P.; Johnston, K. P.; Westacott, R. E.; Rossky, P. J. *J. Phys. Chem. B* **2001**, *105*, 12092.
(27) Allen, M. P.; Tildesley, D. J. *Computer simulations of liquids*; Oxford University Press: New York, 1987.
(28) Liu, Y.; Ichiye, T. *Chem. Phys. Lett.* **1996**, *256*, 334.
(29) Rick, S. W. *J. Chem. Phys.* **2004**, *120*, 6085.
(30) Ren, P.; Ponder, J. W. *J. Phys. Chem. B* **2003**, *107*, 5933.
(31) Guardia, E.; Marti, J. *Phys. Rev. E* **2004**, *69*, 011502.
(32) Flyvbjerg, H.; Petersen, H. G. *J. Chem. Phys.* **1989**, *91*, 461.
(33) Moriyoshi, T.; Kita, T.; Uosaki, Y. *Ber. Bunsen-Ges. Phys. Chem.* **1993**, *97*, 589.
(34) Nxumalo, L. M.; Ford, T. A. *J. Mol. Struct.* **1994**, *327*, 145.
(35) Fennell, C. J.; Gezelter, J. D. *J. Chem. Phys.* **2004**, *120*, 9175.
(36) Svischev, I. M.; Kusalik, P. G. *J. Chem. Phys.* **1993**, *99*, 3049.